HIV-1 Protease: Characterization of a Catalytically Competent Enzyme−Substrate Intermediate

David J. T. Porter,* Mary H. Hanlon, and Eric S. Furfine

GlaxoSmithKline, V297.1C, 5 Moore Drive, Research Triangle Park, North Carolina 27709

Received August 13, 2001; Revised Manuscript Received October 29, 2001

ABSTRACT: The steady-state and pre-steady-state kinetic parameters for the interaction of E with the fluorogenic substrate 2-aminobenzoyl-Thr-Ile-Nle-Phe(p-NO_2)-Gln-Arg-NH_2 were determined in 1.25 M NaCl, 0.1 M MES−TRIS at pH 6.0 at 25 °C. At low concentrations of enzyme, the values of the K_m and k_{cat} calculated from steady-state data were 2.1 μM and 7.4 s^{-1}, respectively. At high concentrations of enzyme, the time-courses of fluorescence enhancement associated with catalysis were very dependent on the excitation wavelength used to monitor the reaction. Because the absorbance spectrum of the substrate overlapped the fluorescence emission spectrum of the enzyme, these abnormalities were attributed to fluorescence energy transfer between the enzyme and the substrate in an enzyme−substrate intermediate. The kinetic data collected with $\lambda_{ex} = 280$ nm and $\lambda_{em} > 435$ nm were analyzed according to the following mechanism in which EX was the species with enhanced fluorescence relative to substrate or products:

$$E + S \overset{K}{\rightleftharpoons} ES \underset{k_{-2}}{\overset{k_2}{\rightleftharpoons}} EX \xrightarrow{k_3} E + P$$

The values of the kinetic parameters with ^1H_2O as the solvent were $K = 13$ μM, $k_2 = 150$ s^{-1}, $k_{-2} = 25$ s^{-1}, and $k_3 = 11$ s^{-1}. The values of the kinetic parameters with ^2H_2O as the solvent were $K = 13$ μM, $k_2 = 210$ s^{-1}, $k_{-2} = 12$ s^{-1}, and $k_3 = 4.4$ s^{-1}. These values yielded solvent isotope effects of 2 on k_{cat} and 0.9 on k_{cat}/K_m. From analysis of the complete time-course of the fluorescence change ($\lambda_{ex} = 280$ nm and $\lambda_{em} > 435$ nm) during the course of substrate hydrolysis, the intermediate EX was determined to be 6.3-fold more fluorescent than the product, which, in turn, was 4.5-fold more fluorescent than ES or S. Rapid quench experiments with 2 N HCl as the quenching reagent confirmed that EX was a complex between enzyme and substrate. Consequently, the small burst in fluorescence observed when monitoring with $\lambda_{ex} = 340$ nm (0.3 product equiv per enzyme equivalent) was attributed to the fluorescence change upon transfer of substrate from an aqueous environment to a nonaqueous environment in the enzyme. These results were consistent with carbon−nitrogen bond cleavage being the major contributor to k_{cat}.

During the course of the development of inhibitors of HIV-1[1] protease as therapeutic agents for AIDS, extensive structural (*1*, *2*), genetic (*3*, *4*), and biochemical (*5*−*10*) characterization of the enzyme have been reported. The enzyme is an aspartyl protease in which the homodimeric active site is composed of an aspartyl group from each monomer (*11*, *12*). The kinetic mechanism of the enzyme has been suggested to be substrate-dependent. For example, substitution of the charged P2′Glu in the substrate Lys-Ala-Arg-Val-Leu-Phe-(*p*-nitro)-Glu-Ala-Nle with a glutamyl residue decreases the substrate efficiency (k_{cat}/K_m) over 95% (*13*). Furthermore, the solvent kinetic isotope effect on the substrate efficiency was eliminated for the less reactive substrate (*13*). These results were interpreted to mean that the rate-limiting step for the more efficient substrate is a chemical step coupled with proton transfer, whereas the rate-limiting step for the less efficient substrate is a conformation change of the enzyme. Meek and co-workers (*5*−*10*) have probed the chemical mechanism of HIV-1 protease for several representative substrates using initial velocity studies, isotope exchange studies, and solvent isotope effects. With Ac-Ser-Gln-Asn-Tyr-Pro-Val-Val-NH_2 as substrate, the kinetic mechanism of Scheme 1 was used to describe the data.

Kinetic evidence for most of the steps in this scheme is lacking. For example, evidence for the isomerization of ES to ES′ is based upon the change in position of the "flaps" observed in crystal structures of apoenzyme and enzyme complexed with inhibitors (*10*, *14*). The final intermediate (EPQ) is included to account for the observed solvent isotope effect on k_{cat} and the lack of a solvent isotope effect on k_{cat}/K_m. The solvent isotope effect was proposed to be the result of protonic shifts in a conformation change or product release step and may not be indicative of a rate-limiting step involving chemistry (*9*).

The studies described herein were directed toward providing kinetic evidence for the isomerization steps depicted in Scheme 1 and toward characterizing the intermediate EX accumulating during catalysis. 2-Aminobenzoyl-Thr-Ile-Nle-Phe(p-NO_2)-Gln-Arg-NH_2, which was different from the substrates used by Meek and co-workers, was chosen as a

* To whom correspondence should be addressed. Tel: (919) 483-4390. FAX: (919) 483-3895. E-mail: djp39807@GlaxoWellcome.com.

[1] Abbreviations: HIV-1, human immunodeficiency virus, type 1; S, 2-aminobenzoyl-Thr-Ile-Nle-Phe(p-NO_2)-Gln-Arg-NH_2; MES, 2-(morpholino)ethanesulfonic acid; TRIS, tris(hydroxymethyl)aminomethane; E, catalytically active dimeric form of HIV-1 protease; P, products of enzymatic hydrolysis of S.

10.1021/bi0116543 CCC: $22.00
Published on Web 12/28/2001

Scheme 1: Simplified Kinetic Mechanism for Substrate Hydrolysis

$$E + S \rightleftharpoons ES \rightleftharpoons ES' \rightleftharpoons EX \rightarrow EPQ \rightarrow E + P + Q$$

model substrate for these studies because (1) product formation could be monitored continuously in a spectrofluorometric assay (*15*) and (2) the excitation wavelength of the substrate was similar to the emission wavelength of the enzyme such that the possibility of fluorescence resonance energy transfer existed (*16*). The latter property resulted in the spectrofluorometric detection of an enzyme−substrate complex that was kinetically competent for catalysis.

MATERIALS AND METHODS

Materials. ULTRA MES and TRIS buffers were purchased from Sigma Chemicals. Amprenavir was from GlaxoSmithKline Compound Stores. The enzyme was purified from *Escherichia coli* containing a construct as described previously (*17*). The enzyme was stored as 100 μL samples at −80 °C in 50 mM HEPES at pH 7.0, 10% glycerol, 5% ethylene glycol, 175 mM imidazole, and 1 mM β-mercaptoethanol (enzyme buffer). The substrate [2-aminobenzoyl-Thr-Ile-Nle-Phe(*p*-NO_2)-Gln-Arg-NH_2,S] and the products [2-aminobenzoyl-Thr-Ile-Nle and Phe(*p*-NO_2)-Gln-Arg-NH_2] were purchased from Bachem or Enzyme System Products. Other chemicals were purchased from commercial sources as ACS reagent grade.

General Methods. The standard buffer was 0.1 M MES−TRIS, 1.25 M NaCl at pH 6.0. The standard temperature was 25 °C. Steady-state fluorescence data were collected with a Kontron SFM 25 spectrofluorometer. Product was monitored with λ_{ex} = 280 or 340 nm and λ_{em} = 420 nm. Rapid reactions were monitored with an Applied Photophysics SX.17MV Spectrophotometer (Leatherhead, U.K.) with λ_{ex} = 280 or 340 nm and λ_{em} > 435 nm. Fluorescence time-courses presented were representative of at least three experiments. The concentration of enzyme was determined by titration of enzymatic activity with amprenavir whose concentration was determined spectrophotometrically (ϵ_{265} = 16.7 mM^{-1} cm^{-1} in 0.1 N NaOH). Enzyme concentrations were expressed in terms of amprenavir binding sites. Dimethyl sulfoxide solutions of substrate and products were prepared gravimetrically. The concentration of substrate in this solution was determined by quantitative amino acid analysis to be 75% of that expected. This correction was applied to all values presented herein. Equations described below were fitted to the data by nonlinear least squares using SigmaPlot from Jandel Scientific (Corte Madera, CA). The fits of the parameters to the data are reported as the fitted value with the standard error of the least significant figure in parentheses.

The effect of heavy water (99%) on the kinetic parameters was determined. After addition of buffer salts, the deuterium oxide content of the reaction was greater than 95%. The p^2H values of these mixtures were determined potentiometrically according to the relationship p^2H = pH meter reading + 0.4 (*18*).

Analysis of Product Progress Curves. The time-courses for the fluorescence change associated with hydrolysis of substrate were multiphasic events when the enzyme concentration was greater than 0.3 μM. The approach to the steady-state was described by eq 1:

Scheme 2: Kinetic Mechanism Describing Substrate Hydrolysis

$$E + S \overset{K}{\rightleftharpoons} ES \underset{k_{-2}}{\overset{k_2}{\rightleftharpoons}} EX \xrightarrow{k_3} E + P$$

$$\Delta F([S],t) = \Delta F([S])(1 - e^{-k_{obs}([S])t}) + v_f([S])t \quad (1)$$

where $\Delta F([S],t)$ was the change in fluorescence at time t for the indicated substrate concentration, $\Delta F([S])$ was the amplitude of the fluorescence change at the indicated substrate concentration, $k_{obs}([S])$ was the pseudo-first-order rate constant describing the time-course of the fluorescence change at the indicated substrate concentration, and $v_f([S])$ was the steady-state rate of fluorescence change at the given substrate concentration. The velocity determined in fluorescence units per second [$v_f([S])$] was converted to micromolar product per second [$v([S])$] by dividing the former value by the response factor (fluorescence units per micromolar), which was determined empirically for the instrument settings for the particular experiment.

The dependence of these parameters on substrate concentration was analyzed in terms of Scheme 2.[2] The fluorescence [$F([S],t)$] generated by the reaction of S with E (λ_{ex} =280 nm, λ_{em} > 435 nm) was attributed to the accumulation of P and EX (eq 2a) where F_P and F_{EX} were the response factors for P and EX, respectively.

$$\Delta F([S],t) = F_P[P([S],t)] + F_{EX}[EX([S],t)] \quad (2a)$$

Assuming that the first step of the reaction described by Scheme 2 was a rapid equilibrium process (K), equations for the time-courses for EX and P formation (eqs 2b,c) were derived for Scheme 2 in a manner analogous to that described for other systems (*19*).

$$[EX([S],t)] = \frac{\frac{k_2[S][E_t]}{(K + [S])}}{\left(\frac{k_2[S]}{(K + [S])} + k_{-2} + k_3\right)}(1 - e^{-(k_2[S]/(K+[S]) + k_{-2} + k_3)t}) \quad (2b)$$

$$[P([S],t)] = \frac{\frac{k_2k_3[S][E_t]t}{(K + [S])}}{\left(\frac{k_2[S]}{(K + [S])} + k_{-2} + k_3\right)} + \frac{\frac{k_2k_3[S][E_t]}{(K + [S])}}{\left(\frac{k_2[S]}{(K + [S])} + k_{-2} + k_3\right)^2}(e^{-(k_2[S]/(K+[S]) + k_{-2} + k_3)t} - 1) \quad (2c)$$

The values given by eqs 2a−c were related to the measured values of $\Delta F([S])$, $k_{obs}([S])$, and $v([S])$ (eq 1) by eqs 3a−d. Because the value of F_{EX} was much greater than that for F_P

[2] Because independent steady-state experiments demonstrated that the K_i values for the products were greater than 50 μM, product inhibition was not included in Scheme 2.

(see Results), the value of $\Delta F([S])$ was essentially determined by EX accumulation (eq 3a).

$$\Delta F([S]) \approx \frac{\Delta F_{\infty}[S]}{\frac{K(k_{-2}+k_3)}{k_2+k_{-2}+k_3}+[S]} \quad (3a)$$

The expression for calculation of the constant term ΔF_{∞} is given by eq 3b.

$$\Delta F_{\infty} = \frac{F_{EP}[E_t]k_2}{k_2+k_{-2}+k_3} \quad (3b)$$

The expressions for $k_{obs}([S])$ and $v([S])$ are given by eqs 3c and 3d, respectively.

$$k_{obs}([S]) = k_{-2}+k_3+\frac{k_2[S]}{K+[S]} \quad (3c)$$

$$v([S]) = \frac{k_3k_2[S][E_t]}{(K(k_{-2}+k_3)+(k_2+k_{-2}+k_3)[S])} \quad (3d)$$

Equations 3a−d were fitted globally to the values measured for $\Delta F([S])$, $k_{obs}([S])$, and $v([S])$.

An independent set of time-courses for product formation was analyzed with the program Dynafit (*20*) and Scheme 2. In addition to the parameters of Scheme 2, the response factors for the fluorescence of EX and P were optimized. For this analysis, the initial equilibrium constant (K in Scheme 2) was defined by the kinetic constants k_{-1} and k_1. The value of k_1 was fixed to an arbitrarily large value of 100 μM^{-1} s^{-1} (*21*).

Rapid Quench and Chase Kinetics. Quench and chase experiments were performed using a RQF-3 Quench-Flow rapid mixer apparatus (KinTeK). The specifications of the instrument were confirmed with the model reaction (hydrolysis of benzylidenemalononitrile) described by KinTek (www.kintek-corp.com). The enzyme (4.8 μM) was mixed initially with an equal volume of 11.2 μM S. This solution was aged for selected times prior to quenching the reaction with an equal volume of 4 N HCl or to chasing the reaction with an equal volume of 120 μM amprenavir. For the quench experiments, the effluent from the Rapid Quench instrument was collected in 1 mL of a mixture of potassium acetate, HCl, and amprenavir such that the final concentrations of reagents in the quenched sample were 1 N HCl, 2 M potassium acetate, and 60 μM amprenavir. The final pH was approximately 5.0. For the chase experiments, the effluent from the Rapid Quench instrument was collected in a total volume of 1 mL containing 60 μM amprenavir. The fluorescence of the product was measured within 15 min with $\lambda_{ex} = 340$ nm and $\lambda_{em} = 420$ nm. The concentrations of product in the samples were calculated by equating the fluorescence value after a 20 s reaction with enzyme to the amount of product formed from complete hydrolysis of S. During the course of the Rapid Quench experiment, the enzyme experiences turbulent flow. Kuzmic has reported that rigorous mechanical stirring inactivated the enzyme (*21*). Consequently, the steady-state activity of the enzyme in the Rapid Quench experiment was taken to be equal to enzyme that survived turbulent flow during the first mixing cycle. The concentration of active enzyme, which was less than 50% of the starting value, was calculated from the steady-state rate.

The predicted time-courses of product formation for the quench experiment and the chase experiment were simulated for Scheme 2 by the Dynafit program where X in EX was assumed to be product or substrate.

RESULTS

Kinetics of Hydrolysis of S by HIV-1 Protease. Hydrolysis of S by HIV-1 protease is associated with a 4.5-fold increase in fluorescence ($\lambda_{ex} = 340$ nm and $\lambda_{em} = 420$ nm) that is used to monitor product formation continuously (*15*). The K_m value of the enzyme for S is dramatically decreased by high salt concentration (*5*, *22*). For the studies described herein, a salt concentration of 1.25 M NaCl was chosen because it yielded a K_m value convenient for mechanistic studies. The progress curve for product formation with 0.014 μM E and 5.6 μM S was described with $k_{cat} = 7.4$ (6) s^{-1} and $K_m = 2.1$ (1) μM (Figure 1A). The progress curves for product formation that was calculated from data collected with excitation wavelengths of 280 and 340 nm were similar (Figure 1A).

In contrast to these results, the time-courses for the fluorescence changes associated with S hydrolysis by 2.4 μM enzyme were very dependent upon the excitation wavelengths. With $\lambda_{ex} = 340$ nm, a small burst in fluorescence (<10% of the total change) was observed whereas with $\lambda_{ex} = 280$ nm a large burst in fluorescence (>80% of the total change) was observed (Figure 1B). The overshoot in fluorescence observed with $\lambda_{ex} = 280$ nm suggested that an enzyme−substrate complex or enzyme−product complex with enhanced fluorescence relative to product accumulated transiently.

Concentration Dependence of the Pre-Steady-State Reaction of S with E with $\lambda_{ex} = 280$ nm and $\lambda_{em} > 435$ nm. The time-course of the fluorescence change associated with the interaction of S with E during the initial 0.2 s of the reaction was described by eq 1 (Figure 1B, inset). The dependence of the parameters of eq 1 on substrate concentration was determined at lower enzyme concentration (0.37 μM) such that initially [S] ≫ [ES] for all concentrations of S used (Figure 2). This concentration of E was sufficiently low that an overshoot in fluorescence (Figure 1B) was not observed in these experiments. Because the value of k_{obs} for the approach to the steady-state had a limiting value at high substrate concentrations (Figure 2, inset), a minimal model to describe these data was that given in Scheme 2. Assuming that the initial binding of S to enzyme was rapid relative to the other steps, the interaction of substrate with E is described by eqs 3a−d. These equations were fitted globally to these data to give $K = 13$ (3) μM, $k_2 = 150$ (2) s^{-1}, $k_{-2} = 25$ (2) s^{-1}, $k_3 = 11$ (1) s^{-1}, and $\Delta F_{\infty} = 0.9$ (2) V. The solid lines in Figure 2 were calculated with the values for these parameters and eqs 3a−d. The values of k_{cat} (9.1 s^{-1}) and K_m (2.4 μM) calculated from these data were similar to those values calculated from data collected at low enzyme concentrations with a conventional spectrofluorometer (7.4 s^{-1} and 2.1 μM, respectively).

A similar data set was collected with ^2H_2O as solvent. These data were analyzed analogously to those collected with ^1H_2O as solvent. The values of the kinetic parameters are summarized in Table 1.

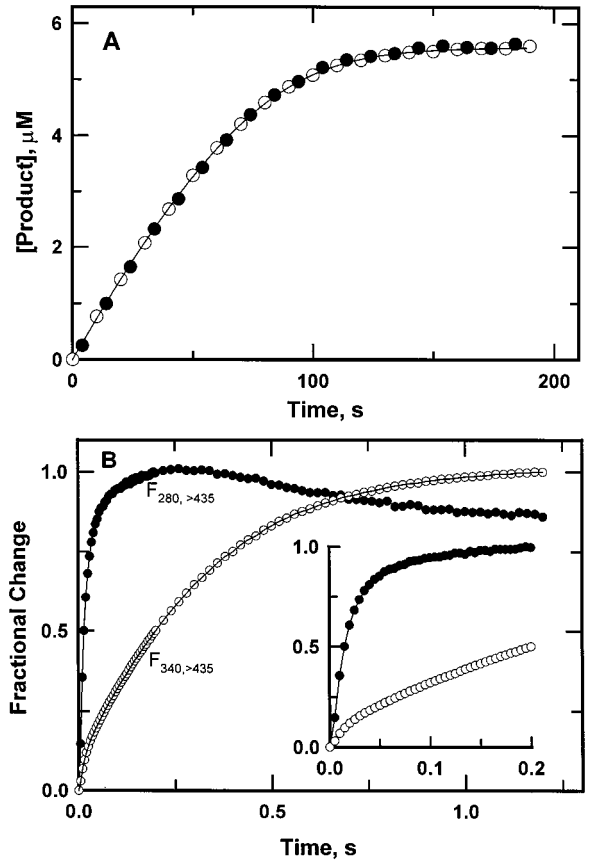

FIGURE 1: Time-courses for hydrolysis of substrate by enzyme. Panel A: Time-course for hydrolysis of 5.6 μM substrate by 0.014 μM E. The reaction was monitored on a conventional spectrofluorometer with $\lambda_{ex} = 340$ nm and $\lambda_{em} = 420$ nm (open circles) and $\lambda_{ex} = 280$ nm and $\lambda_{em} = 420$ nm (closed circles). The fluorescence change has been normalized to the maximal change that corresponded to hydrolysis of 5.6 μM S. The solid line corresponds to the time-course for the hydrolysis of 5.6 μM S by 0.014 μM E with $k_{cat} = 7.40$ (6) s^{-1} and $K_m = 2.1$ (1) μM. Panel B: Time-course for hydrolysis of 5.6 μM substrate by 2.4 μM E. The reaction was monitored with a stopped-flow spectrofluorometer with $\lambda_{ex} = 340$ nm and $\lambda_{em} > 435$ nm (open circles) and $\lambda_{ex} = 280$ nm and $\lambda_{em} > 435$ nm (closed circles). The initial 0.2 s of the reactions is presented in the inset. Equation 1 was fitted to the time-courses of the inset. With $\lambda_{ex} = 280$ nm, the solid curve was calculated with $\Delta F = 0.9$ relative fluorescence unit, $k_{obs} = 52$ s^{-1}, and $v_f = 0.5$ relative fluorescence unit s^{-1}. With $\lambda_{ex} = 340$ nm, the solid curve was calculated with $\Delta F = 0.14$ relative fluorescence unit, $k_{obs} = 43$ s^{-1}, and $v_f = 1.8$ relative fluorescence units s^{-1}.

Analysis of the Complete Time-Course for Hydrolysis of S by E with $\lambda_{ex} = 280$ nm and $\lambda_{em} > 435$ nm. The complete time-course of the reaction of S with E was also analyzed to confirm that the constants derived from steady-state and pre-steady-state data accurately described the reaction. The model of Scheme 2 and the program Dynafit (*20*) were used for this analysis.[2] The fluorescence of S and ES were assumed to be equal, whereas the fluorescence of EX and P were optimized parameters. Fit of this model to the data of Figure 3 yielded $K = 17$ (2) μM, $k_2 = 120$ (1) s^{-1}, $k_{-2} = 21$ (1) s^{-1}, and $k_3 = 18$ (1) s^{-1} with the fluorescence of EX and P at 2.28 (6) V μM^{-1} and 0.362 (1) V μM^{-1}, respectively. The results for the kinetic parameters from this analysis and those obtained from analysis of the pre-steady-state data in eqs 3a−d were in agreement (Table 1). The molar response factor of EX was 6.3-fold larger than that of P.

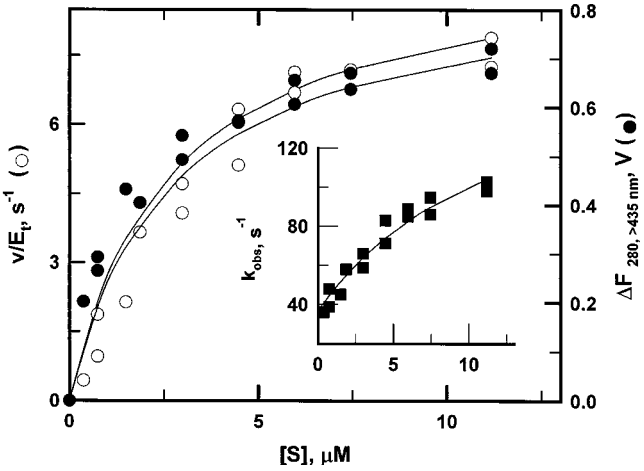

FIGURE 2: Analysis of the fluorescence changes with $\lambda_{ex} = 280$ nm during the hydrolysis of substrate by enzyme. The time-course of the fluorescence increase ($\lambda_{ex} = 280$ nm) during the initial 0.2 s of the reaction of 0.37 μM E with S was a biphasic process described by eq 1. Values for ΔF (closed circles), $v/[E_t]$ (open circles), and k_{obs} (closed squares), which were defined in eq 1, were determined as a function of substrate concentration. The solid lines were calculated (eqs 3a−d) with $K = 13$ μM, $k_2 = 150$ s^{-1}, $k_{-2} = 25$ s^{-1}, $k_3 = 11$ s^{-1}, and $\Delta F_\infty = 0.9$ V.

Table 1: Comparison of the Kinetic Constants for Hydrolysis of S by E in ^1H_2O and ^2H_2O

kinetic constants[a]	^1H_2O[b]	^1H_2O[c]	^2H_2O[b]
K	13 (3) μM	17 (2) μM	13 (2) μM
k_2	150 (2) s^{-1}	120 (1) s^{-1}	210 (1) s^{-1}
k_{-2}	25 (2) s^{-1}	21 (1) s^{-1}	12 (2) s^{-1}
k_3	11 (1) s^{-1}	18 (1) s^{-1}	4.4 (2) s^{-1}

[a] Kinetic constants are defined by Scheme 2 under Materials and Methods. [b] Values of the parameters determined by fitting eqs 3a−d to the pre-steady-state data. [c] Values of the parameters determined by fitting Scheme 2 to a series of progress curves with Dynafit as described under Materials and Methods.

Nature of the Intermediate EX in Scheme 2. When $\lambda_{ex} = 340$ nm, the initial phase of the reaction of S with E resulted in a small burst in fluorescence. This could correspond to free product formation (equivalent to ~0.3 mol of product/mol of enzyme) or to perturbation of substrate fluorescence upon isomerization of ES to EX. In support of the latter interpretation, the fluorescence of S was enhanced 1.5-fold upon transfer from water to either ethanol or *N*,*N*-dimethylformamide. Furthermore, formation of EX from E and S was a readily reversible process ($k_{-2} > 0$, Table 1). This result and the observation that the K_i values for both products were large suggested that if S were cleaved in the formation of EX, both products were present in EX. Consequently, EX was either an enzyme−substrate complex or an enzyme−product complex in which both products were associated with the enzyme. To characterize the EX complex further, rapid chase and rapid quench experiments were undertaken. For the rapid chase experiments, the reaction was stopped with the potent competitive inhibitor amprenavir ($K_i \sim 70$ pM). For the rapid quench experiments, the reaction was terminated with 2 N HCl. In the chase experiment, the partitioning of the EX complex between product formation and substrate formation was determined. In the quench experiment, the EX complex would be disrupted instantaneously to yield E and X, where X was substrate or products.

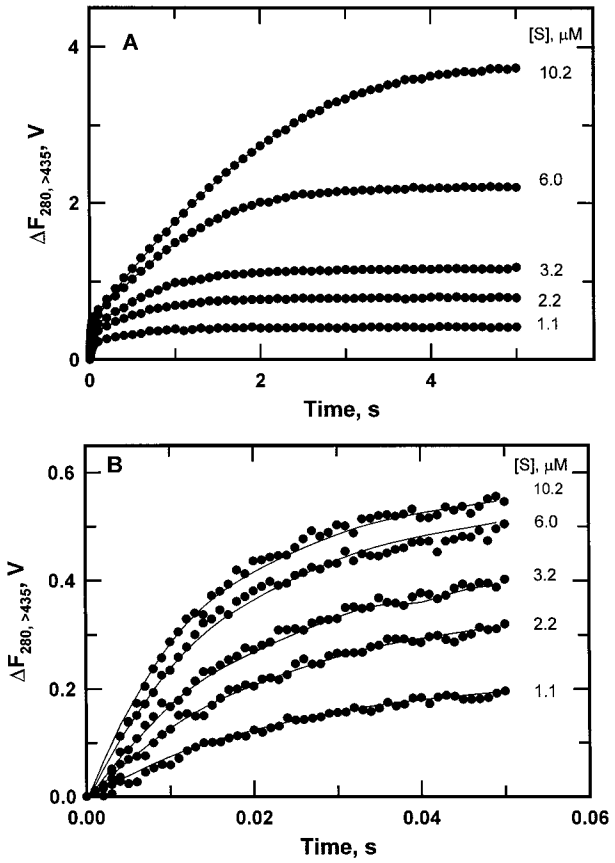

FIGURE 3: Analysis of the time-course for hydrolysis of S by HIV protease. The reaction of 0.56 μM E with the indicated concentrations of S was monitored with the stopped-flow spectrofluorometer and $\lambda_{ex} = 280$ nm and $\lambda_{em} > 435$ nm (panel A and panel B). Scheme 2 was fitted to these data using the Dynafit program. The solid lines were calculated with the values of the parameters given in Table 1. The molar responses of P and EX were 0.362 and 2.28 V μM^{-1}, respectively.

The time-course for product formation with 2.4 μM E with 5.6 μM S followed by 60 μM amprenavir as the chasing reagent was linear for 0.25 s (Figure 4). Similarly, the time-course for product formation with 2 N HCl as the quenching reagent was linear over this time interval (Figure 4). However, the steady-state rate of product formation corresponded to only 1.1 μM active enzyme, whereas the initial concentration of active enzyme was 2.4 μM. This indicated that a significant fraction of the enzyme was inactivated during the initial mixing of enzyme and substrate.

The loss of enzymatic activity upon turbulent mixing of E and S observed in the rapid quench experiment was confirmed in an independent experiment. The enzymatic activity of a sample of 2.4 μM E that was reacted with 5.6 μM S and subsequently quenched with buffer in the rapid quench instrument was compared to that of a sample of enzyme that was diluted with substrate and buffer manually. The enzymatic activity in these samples was determined after a 200-fold dilution into the standard buffer containing 1.9 μM S. Product formation was monitored spectrofluorometrically with $\lambda_{ex} = 340$ nm and $\lambda_{em} = 420$ nm. The activity of enzyme that had passed through the rapid quench instrument was less than 50% of that of untreated enzyme.

Based upon the amount of active enzyme present after the mixing of reagents in the rapid quench apparatus, the time-course for product formation was calculated for the mechanism of Scheme 2 assuming that X was either products or substrate for both the chase and the quench experiments. For the chase experiment, the predicted time-course for product formation was independent of whether X was P or S but was only dependent on the ratio of the values of k_3 and k_{-2} (middle solid tracing of Figure 4). For the quench experiment, the predicted time-course for product formation was dependent on whether X was P or S. If X were P, the predicted time-course for product formation was the upper solid tracing of Figure 4. If X were S, the predicted time-course for product formation was the lower tracing of Figure 4. The data of Figure 4 suggested that X was S.

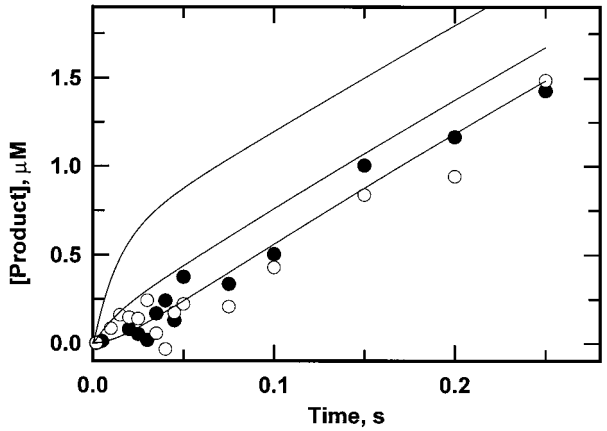

FIGURE 4: Rapid quench experiments to assess the nature of EX in Scheme 2. E (4.8 μM) was mixed with an equal volume of 11.2 μM S in the rapid quench instrument. The reaction was chased or quenched at the indicated times with an equal volume of 120 μM amprenavir (closed circles) or 4.0 N HCl (open circles), respectively. The concentration of product in the mixture was determined fluorometrically as described under Materials and Methods. The amount of active enzyme in the initial reaction was estimated from the steady-state rate to be 1.1 μM. Theoretical time-courses for product formation for the quench experiment were calculated for the mechanism of Scheme 1 and the associated rate constants (Table 1) assuming that X was either P (upper tracing) or S (lower tracing). The theoretical time-course for product formation in the chase experiment was calculated similarly (middle tracing).

DISCUSSION

The data presented herein describe an enzymatic intermediate that accumulates during substrate hydrolysis by HIV-1 protease. The successful detection of this intermediate required the use of high salt (1.25 M NaCl) to decrease the K_m value of the enzyme for substrate and the use of an appropriate fluorescent substrate such that fluorescence resonance energy transfer could occur between E and S. Our kinetic results for the hydrolysis of 2-aminobenzoyl-Thr-Ile-Nle-Phe(p-NO_2)-Gln-Arg-NH_2 by HIV-1 protease are described by Scheme 2. Because the pseudo-first-order rate constant for formation of EX attained a limiting value at high substrate concentrations, an enzyme−substrate complex (ES) formed prior to EX was required for explanation of the data (Scheme 2). The kinetic results demonstrated that formation of EX from ES was a readily reversible process even in the absence of added products. These results suggested that EX either was a complex between enzyme and substrate or was a complex among enzyme and the products of the reaction. The time-course for product formation in an acid quench experiment was consistent with EX being a complex between enzyme and substrate. Furthermore,

because a significant burst in product formation was not observed in a chase experiment, the ratio of k_{-2} to k_3 was greater than 1, which was consistent with the values in Table 1. Aspartic proteases such as pepsin (*23*) catalyze substrate hydrolysis through an iso mechanism in which an isomerized form of resting enzyme accumulates during catalysis. This mechanism predicts a "burst" of product formation during an acid quench experiment. We did not observe a "burst" in product formation during the pre-steady-state phase of the reaction of HIV-1 protease with S. If HIV-1 protease catalyzed S hydrolysis by an iso mechanism, only a small fraction of the total enzyme accumulated as the iso form during catalysis with this substrate. Our results suggested that the enzymatic intermediate accumulating during the enzymatic hydrolysis of substrate (EX in Scheme 2) was a complex of enzyme and substrate with low commitment to catalysis.

The solvent kinetic isotope effects on k_{cat} and k_{cat}/K_m for HIV-1 protease have been used in mechanistic studies of the enzyme (*6*, *9*, *13*). Unfortunately, the magnitude of the effect depends on the substrate. Some substrates expressed a normal solvent isotope effect of k_{cat}/K_m (*13*), whereas others only expressed an effect on k_{cat} (*6*, *13*). A normal solvent isotope effect on the value of k_{cat}/K_m was suggested to indicate that the chemical step of the reaction is rate-limiting (*13*). However, this conclusion is valid only if the commitment to catalysis is low. In general, a solvent isotope effect on k_{cat}/K_m indicates that the steps involving substrate binding and the step expressing the isotope effect are coupled [i.e., not separated by an irreversible step (*9*)]. Rodriguez et al. (*9*) observed that the solvent isotope effect on the hydrolysis of Ac-Ser-Gln-Asn-Tyr-Pro-Val-Val-NH_2 was expressed on k_{cat} and not k_{cat}/K_m. They concluded that the solvent isotope effect was expressed on a reaction step after carbon−nitrogen bond cleavage, such as an isomerization or product release step (*9*). However, the results presented herein for our substrate demonstrate an alternative mechanism for the observation of an isotope effect on k_{cat} and not on k_{cat}/K_m. In this case, the solvent isotope effect occurred on two steps of the reaction. A normal solvent isotope effect of 2 was observed on the major contributor to k_{cat} (k_3 in Scheme 2), and an inverse solvent isotope of 0.4 was observed on the isomerization step immediately prior to the rate-limiting step (the ratio of k_2 to k_{-2} in Scheme 2). This result suggested that protonic movements were involved in the isomerization step ES to EX. Inverse solvent isotopes on substrate−enzyme binding of the magnitude reported here have been observed in other systems (*24*). The values of the solvent isotope effects of k_{cat} and k_{cat}/K_m were calculated from these data to be 2 and 0.9, respectively.

In summary, HIV-1 protease reacted with 2-aminobenzoyl-Thr-Ile-Nle-Phe(*p*-NO_2)-Gln-Arg-NH_2 to give an initial enzyme−substrate complex (ES) that isomerized to a kinetically competent intermediate EX. This intermediate, which was also an enzyme−substrate complex, was the primary enzymatic intermediate accumulating during catalysis. The isomerization of ES to EX must be associated with significant realignment of S with the tryptophanyl residues of the enzyme such that fluorescence resonance transfer was observed. The isomerization step was associated with a significant equilibrium isotope effect. The subsequent processing of EX in the catalytic cycle was also associated with a normal solvent isotope effect. The results of these isotope effects on two adjacent steps of the catalytic cycle were an expressed isotope effect on k_{cat} and an equilibrium isotope effect on K_m such that the isotope effect on k_{cat}/K_m was close to 1. Our results have established that EX is an enzyme−substrate complex and are consistent with k_3 in Scheme 2 being the kinetic step in which carbon−nitrogen bond cleavage occurs.

REFERENCES

1. Wlodawer, A., Miller, M., Jasko'lski, M., Sathyanarayana, B. K., Baldwin, E., Weber, I. T., Selk, L. M., Clawson, L., Schneider, J., and Kent, S. B. H. (1989) *Science 245*, 616−621.
2. Lapatto, R., Blundell, T., Hemmings, A., Overington, J., Wilderspin, A., Wood, S., Merson, J. R., Whittle, P. J., Danley, D. E., Geoghegen, K. F., Hawrylik, S. J., Lee, S. E., Scheld, K. G., and Hobart, P. M. (1989) *Nature (London) 242*, 299−302.
3. Kohl, N. E., Emini, E. A., Schleif, W. A., Davis, L. J., Heimbach, J. C., Dixon, R. A. F., Scolnick, E. M., and Sigal, I. S. (1988) *Proc. Natl. Acad. Sci. U.S.A. 85*, 4686−4690.
4. Peng, C., Ho, B. K., Chang, T. W., and Chang, N. T. (1989) *J. Virol. 63*, 2550−2556.
5. Hyland, L. J., Tomaszek, T. A., Jr., Roberts, G. D., Carr, S. A., Magaard, V. W., Bryan, H. L., Fakhoury, S. A., Moore, M. L., Minnich, M. D., Culp, J. S., DesJarlais, R. L., and Meek, T. D. (1991) *Biochemistry 30*, 8441−8453.
6. Hyland, L. J., Tomaszek, T. A., and Meek, T. D. (1991) *Biochemistry 30*, 8454−8463.
7. Richards, A. D., Phylip, L. H., Farmerie, W. G., Scarborough, P. E., Alvarez, A., Dunn, B. M., Hirel, P.-H., Konvalinka, J., Strop, P., Pavlickova, L., Kostka, V., and Kay, J. (1990) *J. Biol. Chem. 265*, 7733−7736.
8. Grant, S. K., Deckman, I. C., Culp, J. S., Minnich, M. D., Brooks, I. S., Hensley, P., Debouck, C., and Meek, T. D. (1992) *Biochemistry 31*, 9491−9501.
9. Rodriguez, E. J., Angeles, T. S., and Meek, T. D. (1993) *Biochemistry 32*, 12380−12385.
10. Rodriguez, E. J., Debouck, C., Deckman, I. C., Abu-Soud, H., Raushel, F. M., and Meek, T. D. (1993) *Biochemistry 32*, 3557−3563.
11. Babe, L. M., Pichuantes, S., and Craik, C. S. (1991) *Biochemistry 30*, 106−111.
12. Cheng, Y.-S. E., Yin, F. H., Foundling, S., Blomstrom, D., and Kettner, C. A.(1990) *Proc. Natl. Acad. Sci. U.S.A. 87*, 9960−9664.
13. Polgar, L., Szeltner, Z., and Boros, I. (1994) *Biochemistry 33*, 9351−9357.
14. Miller, M., Schneider, J., Sathyanarayana, B. K., Toth, M. V., Marshall, G. R., Clawson, L., Selk, L., Clawson, L., Kent, S. B. H., and Wlodawer, A. (1989) *Science 246*, 1149−1152.
15. Toth, M. V., and Marshall, G. R. (1990) *Int. J. Pept. Protein Res. 33*, 544−550.
16. Selvin, P. R. (1995) *Methods Enzymol. 246*, 300−334.
17. Porter D. J. T., Hanlon, M. H., Carter, L. H., III, Danger, D. P., and Furfine, E. S. (2001) *Biochemistry 40*, 11131−11139.
18. Glasoe, P. K., and Long, F. A. (1960) *J. Phys. Chem. 64*, 188−190.
19. Fersht, A. (1985) *Enzyme Structure and Mechanism*, p 135, W. H. Freeman and Co., New York.
20. Kuzmic, P. (1996) *Anal. Biochem. 237*, 260−273.
21. Kuzmic, P., Peranteau, A. G., Garcia-Echeverria, C., and Rich, D. H. (1996) *Biochem. Biophys. Res. Commun. 221*, 313−317.
22. Wondrak, E. M., Louis, J. M., and Oroszlan, S. (1991) *FEBS Lett. 280*, 344−346.
23. Cho, Y. K., Rebholz, K. L. and Northrop, D. B. (1994) *Biochemistry 33*, 9637−9642.
24. Cho, Y. K., and Northrop, D. B. (2000) *Biophys. J. 79*, 1621−1628.

BI0116543